

Cloning and biological activity of an anti-tumor peptide of Tumstatin

WANG Shujing^{1,2,3}, LIU Yan^{1,2}, LIN Xuesong^{1,2}, FU Xue^{1,2}, XU Jianyong^{1,2}, LIU Xinghan (✉)^{1,2}

1 Bio-pharmaceutical Key Laboratory of Heilongjiang Province—Incubator of State Key Laboratory, Harbin Medical University, Harbin 150086, China

2 Department of Biochemistry and Molecular Biology, Harbin Medical University, Harbin 150028, China

3 Institute of Pharmacology, Harbin Commercial University, Harbin 150028, China

© Higher Education Press and Springer-Verlag 2007

Abstract To obtain an anti-tumor peptide of Tumstatin and detect its biological activity, the nucleotide sequence encoding 185–203 amino acids (19peptide) of Tumstatin was synthesized and inserted into the fusion protein vector pTYB2. After identification by sequencing and restriction endonucleases, the recombinant vector was transformed into BL-21 (DE3) *E. coli* competent cells. Transformed *E. coli* BL-21 (DE3) were induced by isopropyl- β -thiogalactopyranoside (IPTG), and then expressed. By 1,4-dithiothreitol (DTT) reduction, the soluble 19peptide was obtained from a chitin affinity chromatograph. The biological activity of 19peptide was determined by 3-[4,5-dimethylthiazol-2-yl]-2,5-diphenyltetrazolium bromide (MTT) assay, cell growth curve, the effect of the ascitic fluid transfevent H22 hepatoma on mice and via histopathological slices. The purified 19peptide directly inhibited proliferation and migration of murine B16 melanoma cells, SMMC-7721 hepatoma carcinoma cells and human umbilical vein endothelial cells (HUVEC). The tumor inhibition rate of mice ascitic fluid transfevent H22 hepatoma was 48.46%. Histopathological slices showed that it could promote tumor tissue necrosis and decrease the density of blood vessels. With higher anti-tumor activity, 19peptide has the potential to become a novel, potent anti-tumor agent.

Keywords Tumstatin; protein expression; protein purification; tumor therapy

1980s (Saus et al., 1988; Colorado et al., 2000). By 2000, Kamphaus found that it had two distinct anti-tumor domains that had direct and indirect anti-tumor effects, respectively (Maeshima et al., 2000; Ortega and Werb, 2002). The 78peptide comprising of amino acids from 54 to 132 near its N termini had an anti-angiogenesis effect. The 19peptide comprised of amino acids from 185 to 203 near its C termini can directly repress the proliferation of tumor cells. It can bind the integrin $\alpha v \beta 3$ to mediate the intercellular interaction independent of Vitronectin, Fibronectin and RGD sequences (Kalluri, 2002; Kumar, 2003). That is, it can repress the adhesion, tendency and accrementation of different tumor cells such as melanoma cells, fibroma cells and polymorphonuclear leucocytes (Maeshima et al., 2001).

As part of the whole Tumstatin, 19peptide could not display anti-tumor activity, the reasons of which may be that the active region was covered and not able to bind to receptors such as integrin $\alpha v \beta 3$. Thus, we designed and artificially synthesized the base sequence of 19peptide (Tum19) and inserted Tum19 into the fusion protein vector pTYB2. The 19peptide was then expressed in *E. coli* BL-21(DE3) and purified with chitin affinity chromatograph. Finally, the soluble 19peptide was obtained and the initial research was carried out on its anti-tumor activity.

1 Introduction

Tumstatin, an NC1 domain fragment of the type IV collagen $\alpha 3$ chain, was discovered as a good-pasture antigen in the

Translated from *Chinese Journal of Biochemistry and Molecular Biology*, 2005, 21(3): 322–328 [译自: 中国生物化学与分子生物学学报]

E-mail: lxlxhs@163.com

2 Methods

2.1 The design and synthesis of the gene

According to the amino acids of 19peptide and the codon *E. coli* favored, the gene of 19peptide was designed to enhance its expression level in genetic engineering bacteria. The 3'-termini of the designed gene (Tum19) was blunt to link to the 5'-termini of the intein gene, which was one part of the fusion

protein pTYB2 vector. The 5'-termini had *NdeI* restriction site TATG, containing the translation initiation codon. The amino acid sequence, biological activity and other characteristics of Tum19 had not changed after it was reconstructed. Tum19 synthesis was done using a DNA synthesizer. The nucleotide sequence is as follows:

5'-T A T G GCT AGC CCT TTC CTA GAA TGT CAT
GGA AGA GGA ACG TGC AAC TAC TACTCA AAC
TCC-3'

3'-AC CGA TCG GGA AAG GAT CTT ACA GTA CCT
TCT CCT TGC ACG TTG ATG ATGAGT TTG AGG-5'

2.2 Construction of engineering bacteria

The synthesized gene of 19peptide (Tum19) was phosphorylated and annealed until it became a double stranded DNA. The vector pTYB2 (NEB Corporation) was cleaved by *NdeI* and *SmaI* restriction endonucleases (Promage Corporation), following the manufacturer's recommendations. After Tum19 and reconstructed vector pTYB2 was purified using the silver beads gel DNA extraction kit (Shanghai Sangon Biological Engineering Technology), pTYB2 vector was ligated to Tum19. The recombined plasmid was transformed by JM109 *E. coli* competent cells (Promage Corporation) and was identified by means of *NdeI* and *XhoI* endonucleases. After that, it was submitted to Boya Biological Engineering Technology for sequencing.

2.3 Protein expression and purification

Tum19 recombined with the pTYB2 vector was transformed in BL-21 (DE3) *E. coli* competent cells. Transformed *E. coli* were plated on Luria Bertani (LB) agar plates containing $100 \mu\text{g} \cdot \text{mL}^{-1}$ of ampicillin and incubated at 37°C for 14–18 h. Isolated colonies on the agar plates were selected and used to inoculate 10 mL of LB media containing $100 \mu\text{g} \cdot \text{mL}^{-1}$ of ampicillin, which was maintained in a rotary culture at 37°C overnight. Then, 5 mL of transformed culture was used to inoculate 250 mL of LB media containing $100 \mu\text{g} \cdot \text{mL}^{-1}$ of ampicillin (culture:LB = 1:50). This large-scale culture was maintained at 37°C until it reached an optical density ($\text{OD}_{600} = 0.5$). Protein expression was induced by IPTG (TakaRa Corporation) at a final concentration of $0.1 \text{ mmol} \cdot \text{L}^{-1}$, 28°C , 6 h. Induced cells were harvested by centrifugation at 5,000 g. Prior to protein purification, the cell pellet was thawed on ice and resuspended in phosphate buffer (50 mM NaH_2PO_4 , 10 mM imidazole and 2.5 M NaCl, pH 8) containing lysozyme at a concentration of $100 \mu\text{g} \cdot \text{mL}^{-1}$, and the solution was incubated on ice for 30 min. Following enzymatic lysis, the cells were sonicated for six cycles of 10 s each and then centrifuged at 19,000 g for 30 min at 4°C . The lysate supernatant was harvested and introduced into chitin-affinity column (NEB Corporation). The method of purification follows the article (Yu et al., 2004).

2.4 Protein activities determination

2.4.1 MTT assay

About 5,000 murine B16 melanoma cells were cultured in 96-well plates and allowed to reach 30% confluency. All cells were maintained in a RPMI1640 cell culture medium supplemented with 10% fetal calf serum (FCS) at 37°C and 5% CO_2 . After the cells were allowed to equilibrate for 24 h, growth media were replaced with media containing purified 19peptide at concentrations of $44 \mu\text{g} \cdot \text{mL}^{-1}$, $88 \mu\text{g} \cdot \text{mL}^{-1}$, $132 \mu\text{g} \cdot \text{mL}^{-1}$, $176 \mu\text{g} \cdot \text{mL}^{-1}$, $220 \mu\text{g} \cdot \text{mL}^{-1}$ and six wells were arranged for each concentration. Following the addition of 19peptide, the murine B16 melanoma cells were maintained for an additional 48 h at 37°C in 5% CO_2 . After this final incubation, 100 mL of a $25 \text{ mg} \cdot \text{mL}^{-1}$ solution of MTT was added to each well and allowed to incubate at room temperature for 1 h. The media were then removed, and the resulting purple formazan precipitate was resolubilized with 200 mL of dimethyl sulphoxide (DMSO) (TakaRa). The wells were evaluated spectrophotometrically at a wavelength of 490 nm. The amount of light absorption (A_{490}) directly correlates with cell survival. A well containing only DMSO served as the blank for background light absorption. The amount of light absorbed by control cells not exposed to 19peptide was used to define 100% survival. The relative cell survival for each concentration of 19peptide evaluated can be calculated. The MTT assay was also performed on hepatoma carcinoma cells and human umbilical vein endothelial cells (HUVEC) using the methods described above.

2.4.2 Cell growth curve

Murine B16 melanoma cells in good condition were digested by 0.5% pancreatic protease and cell supernatant was made following conventional methods. About 1.5×10^4 murine B16 melanoma cells were cultured in 24-well plates. All cells were maintained in a RPMI1640 cell culture medium supplemented with 10% fetal calf serum (FCS) at 37°C and 5% CO_2 . The cells were allowed to equilibrate for 24 h. Experimental wells were replaced with media containing purified 19peptide at a concentration of $44 \mu\text{g} \cdot \text{mL}^{-1}$. The control wells were added with the same volume growth media PBS as the experimental wells. Following the addition of 19peptide, we took 3 wells each of the experimental group and the control group daily, to count the live cells and derived the mean value for 6 days, then drew cell growth curves. Cell growth curves were also performed on hepatoma carcinoma cells and human umbilical vein endothelial cell (HUVEC) using the methods described above.

2.4.3 Cell morphology

Murine B16 melanoma cells in good condition were digested by 0.5% pancreatic protease and cell supernatant was made following conventional methods. About 1.5×10^4 murine B16

melanoma cells were cultured in 6-well plates. All cells were maintained in a RPMI1640 cell culture medium supplemented with 10% FCS at 37°C and 5% CO₂. At the same time, microscopic glass was put in every well. After the cells were allowed to equilibrate for 24 h, experimental wells were replaced with media containing purified 19peptide at a concentration of 22 μg · mL⁻¹ and the same volume of growth media PBS was also added to the control wells. After 48 h, each microscopic glass was taken out for hematoxylin-eosin (HE) staining. Cell morphology of murine B16 melanoma cells were observed under a microscope as soon as the microscopic glass was dried at 37°C. Cell morphology was also performed on hepatoma carcinoma cells and HUVEC using the methods described above.

2.4.4 The experiment of mice tumor inhibition

The frozen mice H22 hepatoma carcinoma cells were put in water at 37°C for 1–2 min. As soon as it was melting, we took 0.2 mL of that and injected it into the mice abdominal cavity. After 10 days, we extracted the ascites and adjusted the density of living cells to 3 × 10⁷ mL⁻¹ and injected 0.15 mL hypodermically on the right foreleg armpit of 24 male Kunming mice weighing 18–22 g. When the hypodermic tubercle could be touched after 3 days, the 24 male Kunming mice were stochastically divided into two groups. The experimental group was injected with 19peptide of 4.3 mg · kg⁻¹ daily, while the control group was injected with the same volume of isometric physiological saline. After 7 days, the mice were executed and each tumor was taken out to measure its length and weight. Meanwhile, each mouse tumor was striped and its histopathological slice was observed under a microscope through conventional paraffin section and HE staining.

3 Results

3.1 Recombined plasmid identification

There was an *Xho*I restriction site between the *Nde*I and *Sma*I restriction sites in native pTYB2 vector. Because the pTYB2 vector ligated to Tum19 would lose the *Xho*I restriction site, we can use the *Xho*I restriction endonuclease to identify

whether Tum19 recombined with pTYB2. On the other hand, native pTYB2 vector cleaved by *Nde*I and *Sma*I restriction endonucleases can be ligated itself with its *Nde*I restriction site destroyed. Therefore, the recombined plasmid could be identified through *Xho*I and *Nde*I restriction endonucleases at first, and then be verified by sequencing. The results were completely consistent with the 19peptide base sequence we designed (Figs. 1, 2).

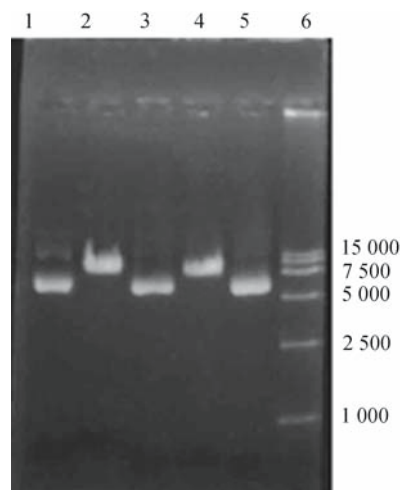


Fig. 1 Electrophoresis of digested recombinant plasmid pTYB2-Tum19
1: pTYB2-Tum19 by *Xho*I; 2: pTYB2-Tum19 by *Nde*I; 3: pTYB2-Tum19; 4: pTYB2 by *Nde*I; 5: pTYB2; 6: Marker

3.2 Protein expression and purification of 19peptide

Recombinant plasmid pTYB2-Tum19 transformed in BL-21 (DE3) was expressed by fusion protein. The protein of pTYB2 vector comprising the intein tag was as much as 484 amino acids. The total amino acids of 19peptide and the pTYB2 vector were 503. The molecular weight of recombinant plasmid pTYB2-Tum19 was about 55 KD. After pTYB2-Tum19 was expressed in BL-21 (DE3), induced by IPTG, cells were broken by sonication. The supernatant was obtained by centrifugation and analyzed by SDS-PAGE. There was an obvious belt on the site of 55 KD. Under the

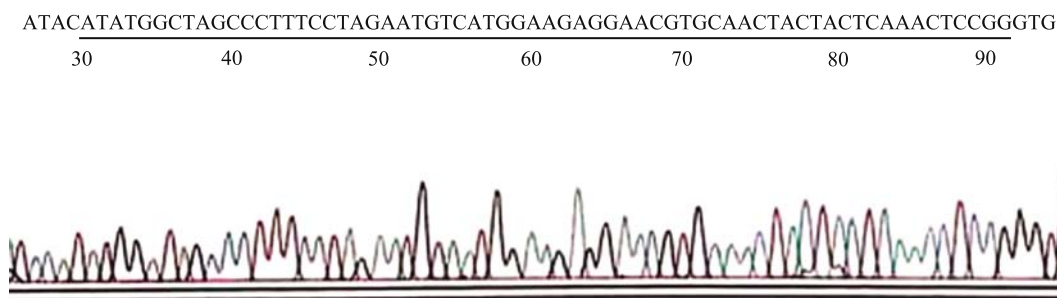


Fig. 2 The local sequencing result of recombinant plasmid pTYB2-Tum19

optical condition 28°C, 0.1 mmol·L⁻¹ IPTG, 6 h, the protein they expressed was as much as 40%. The variable density of IPTG from 0.1 mmol·L⁻¹ to 1.0 mmol·L⁻¹ would not influence protein expression. By DTT reduction, the intein underwent specific self-cleavage, which released the 19peptide from the chitin-bound intein tag resulting in one single-affinity column purification. Due to 19peptide's small molecular weight, it had not been detected on a regular SDS-PAGE gel. However, it can be separated from the fusion protein by DTT reduction. The results of SDS-PAGE gel and curves of affinity chromatography for 19peptide are as follows (Figs. 3, 4)

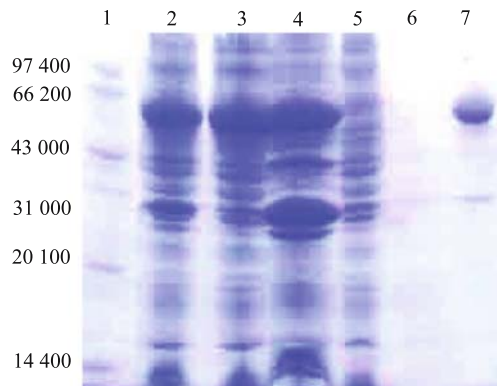


Fig. 3 SDS-PAGE analysis of expression and purification of 19peptide
1: Mark; 2: After induction; 3: Supernatant protein; 4: Precipitation; 5: Mixed protein of *E.coli*; 6: 19peptide; 7: Vector protein

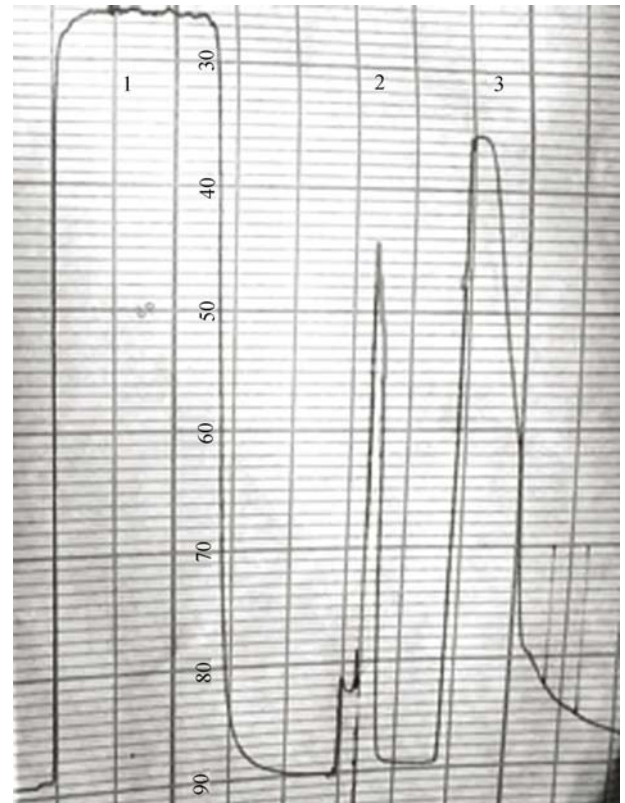


Fig. 4 Curves of affinity chromatography for 19peptide
Peak 1: the mixed protein of *E.coli*; Peak2: 19peptide; Peak 3: vector protein

3.3 19peptide affects cell proliferation and apoptosis in vitro

3.3.1 19peptide affects cell viability

The effects of 19peptide on murine B16 melanoma cell, hepatoma carcinoma cell, and human umbilical vein endothelial cell (HUVEC) viability were evaluated using the MTT assay. The MTT assay demonstrated a significant dose-dependent decrease in the number of viable murine B16 melanoma cells, hepatoma carcinoma cells, and HUVEC after 48 h exposure to 19peptide, relative to the control group. As expected, 19peptide-treated murine B16 melanoma cells and hepatoma carcinoma cells had significantly decreased viable cell populations compared with the control. 19peptide can also decrease HUVEC population to some extent. The relative half cell survival rate of murine B16 melanoma cells, hepatoma carcinoma cells, and HUVEC were 49.45 $\mu\text{g}\cdot\text{mL}^{-1}$, 54.22 $\mu\text{g}\cdot\text{mL}^{-1}$, 45.56 $\mu\text{g}\cdot\text{mL}^{-1}$, respectively.

3.3.2 19peptide affects cell proliferation

19peptide had inhibitory effects on the proliferation of three kinds of cells, especially on murine B16 melanoma cells and

hepatoma carcinoma cells. With 19peptide, we were unable to count the amount of live murine B16 melanoma cells and hepatoma carcinoma cells on the first day and on the third day respectively. But to the endothelial cells, the inhibitory action was not obvious, and only the number of live endothelial cells decreased by half compared with the control group.

3.3.3 19peptide affects cell apoptosis

By HE staining, three kinds of cells with 19peptide were observed for nucleolus condensation, nuclear fragmentation and cell surface with vacuole under oil microscope, which indicated that 19peptide probably can promote apoptosis of the three kinds of cells.

3.4 19peptide induces mice tumor inhibition *in vivo*

In the experiment *in vivo*, mice tumors, whether from the control group or the experimental group, continued to grow. However, the tumors of the experimental group were obviously smaller than those of the control group. Through statistical analysis of tumor weight, the difference between the experimental group and the control group was remarkable at $P < 0.05$. The tumor inhibition rate of ascitic fluid transfevent H22 hepatoma of mice was 48.46%. From the mice tumor

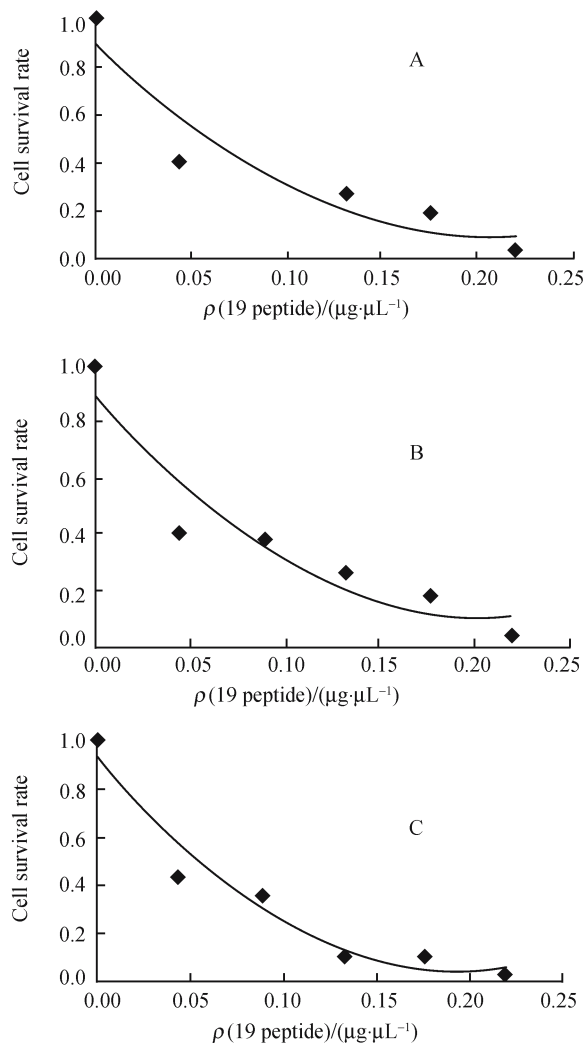


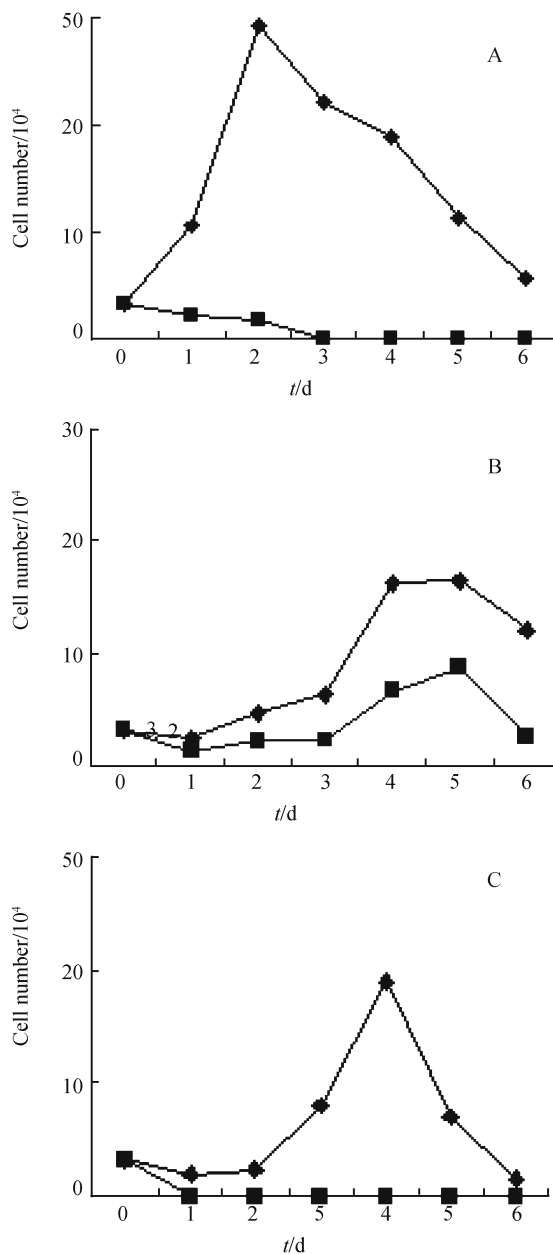
Fig. 5 MTT assay for three kinds of cell

(A) Curve of human SMMC-7721 hepatoma carcinoma cell survival rate and 19 peptide concentration; (B) Curve of HUVEC survival rate and 19 peptide concentration; (C) Curve of murine B16 melanoma cell survival rate and 19 peptide concentration

pathology tissue slice ($\times 20$), we detected that the number of blood vessels was obviously decreased and the tumor tissue appeared as a massive necrosis.

4 Discussion

At present, tumor-therapeutics drugs can be classified into two types according to their target cell (Maeshima et al., 2002; Scappaticci, 2002). One can affect endothelial cells and reach its anti-tumor function via inhibiting the formation of new vessels (Folkman, 1995; O'Reilly et al., 1997). The other is directly aimed at the tumor cell to promote tumor cell apoptosis and inhibit tumor cell proliferation. The former is more and more valuable for its broad anti-tumor spectrum, no poisonous side effect, and no drug reliability, etc. However, it can only inhibit blood vessel formation and cannot promote



Control: \blacklozenge Experiment: \blacksquare

Fig. 6 The growth curve of three kinds of cell

(A) Growth curve of human SMMC-7721 hepatoma carcinoma cell; (B) Growth curve of HUVEC; (C) Growth curve of murine B16 melanoma cell

tumor cell apoptosis directly. With this kind of medicine, the tumor cell only returned to the primary condition due to lack of blood supply. Once medicine intake is stopped, these tumor cells will be able to proliferate again. Therefore, it is significant for tumor-therapy to have the anti-angiogenesis medicine coordinate with a medicine promoting tumor cell apoptosis. Even if anti-angiogenesis has been supplied widely in clinical medication these days, research on anti-tumor medicine with high effectivity, low poisonous side effects, and direct suppression of tumor cell multiplication is still important (Lucas et al., 1998; Scappaticci, 2003).

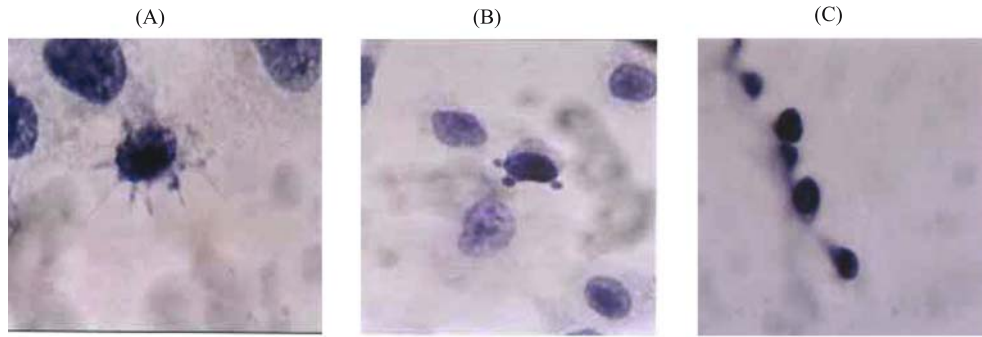


Fig. 7 The result of HE staining of three kinds of cell
(A) Hepatocarcinoma cell; (B) Human umbilical vein endothelial cell; (C) Murine B16 melanoma cell

Table 1 Effect of 19peptide on H22 ascitic fluid transfevent hepatoma of mice growth ($\bar{x} \pm s, n = 12$)

	x_i/g				\bar{x}_i/g		IR/%
Control	1.015 2	3.152 3	2.764 5	2.996 9	2.508 3	2.651 1	$2.514 7 \pm 0.624 7$
	2.432 5	3.071 8	2.894 7	1.796 8	2.035 6	2.856 8	
19peptide	1.422 4	1.701 6	0.654 7	2.189 6	0.861 6	0.947 2	$1.296 2 \pm 0.509 5$
	1.308 0	0.811 6	1.782 2	1.898 0	0.731 5	1.245 9	

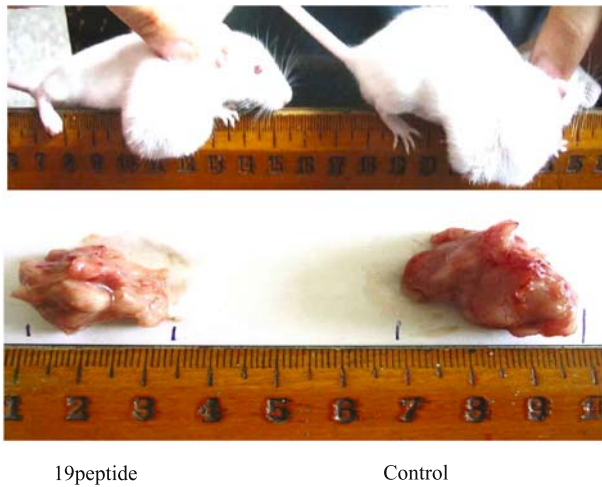


Fig. 8 Effect of 19peptide on H22 ascitic fluid transfevent hepatoma of mice growth

Tumstatin was discovered to promote tumor cell apoptosis in 2000. It is a large molecular weight protein and is an antigen of good-pasture itself, which makes it unsecure in clinical application. Further studies indicated that 19peptide had anti-tumor activity independent of Tumstatin. The active domain of 19peptide was located at 189–191 amino acids, that is -SNS-, which constituted turn structure between two beta pleated sheets (Floguet et al., 2004). If the spatial structure of -SNS- was not variable, 19peptide could maintain its anti-tumor activity (Kalluri et al., 2002). Based on the achievements above, we sought to reconstruct Tumstatin’s structure, and use genetic engineering methods to construct high protein expression *E. coli* gene engineering bacteria. 19peptide was expressed by fusion protein and purified in just one single step of chitin affinity chromatograph. The advantages of this method include minimum loss, high yield of fusion polypeptide, lower cost, and profit in the competitive market,

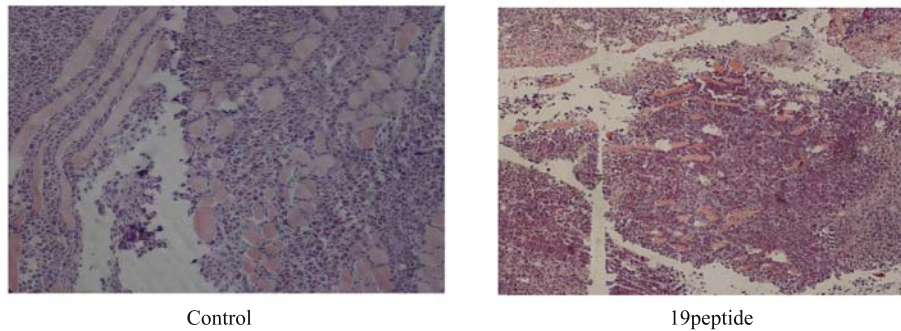


Fig. 9 HE staining of H22 ascitic fluid transfevent hepatoma of mice

which will lay the foundations for its mechanism of action, biological activity and use in clinical tumor therapy.

Because 19peptide has a low molecular weight, it was not detected in a regular SDS-PAGE gel, which made it difficult to detect and identify its concentration, expression and purification. However, the vector pTYB2 and chromatographic analysis matrix (chitin beads) that we used determined when the second peak of chromatographic analysis was coming, and at the same time, what we collected was the purified 19peptide. A280/A260 determination and high performance liquid chromatography detection could derive its density and the rate of purification. The rate of its protein purification was as much as 90.83%. We once used this method to purify and examine the recombinant human osteogenic growth peptide (rhOGP), and the results were satisfactory. The obtained active peptide obviously inhibited murine B16 melanoma cell proliferation, which had also proven that what we obtained was the 19peptide of Tumstatin.

As reported, 19peptide had a strong inhibitory action to murine B16 melanoma cell. Whether it influenced the proliferation of other tumor cells still needs further research to confirm (Maeshima et al., 2000). We had proven that 19peptide suppressed murine B16 melanoma cell and hepatic carcinoma cell multiplication and that it affected the former more greatly. After only 1 day, we were not able to count the number of living cultured murine B16 melanoma cells. On the other hand, living hepatic carcinoma cells reached a similar stage only after the third day with 19peptide, which also showed that 19peptide can affect the proliferation of different tumor cells.

The base sequence of 19peptide is relatively conservative. The mechanism of 19peptide and anti-angiogenesis domain of tum-5 has something in common, which would indicate that 19peptide possibly affected endothelial cell multiplication to inhibit tumor blood vessel production. The HUVEC was chosen to confirm the above prediction (Maeshima et al., 2001; Pasco et al., 2000; Sudhakar et al., 2003). 19peptide displayed certain inhibitory action to HUVEC cell multiplication. Based on cell growth curves, the number of living cells in the experimental group reduced by one half as compared to those in the control group. The number of blood vessels decreased in histopathological slices of mice ascitic fluid transfevent H22 hepatoma, which further confirmed that 19peptide had an inhibitory action on blood vessel formation. The potency of 19peptide in inhibiting vascularization is not well understood.

In this experiment, we made a mice ascitic fluid transfevent H22 hepatoma model and applied it to examine the tumor inhibition effects of 19peptide in animals *in vivo*. In mice with 19peptide at the daily concentration of 4.3 mg/kg, tumor inhibition rate was as much as 48.46% after 7 days. 19peptide suppression of tumor growth *in vitro* was equally remarkable as *in vivo*. Because the mice ascitic fluid transfevent H22 hepatoma model was easy to made, and had relatively even tumor size, we do not have to use nude mice, which makes the cost of the experiment inexpensive. On

the other hand, the sequence of small molecular anti-tumor multi-peptides was mostly conservative. Homology between humans and mice is high. 19peptide does not have specificity in activity. If the laboratory is unable to raise nude mice, culturing tumor cells *in vitro* and mice ascitic fluid transfevent H22 hepatoma can be done to identify its anti-tumor activity. If necessary, human tumor cells and nude mice can be used to carry on further research.

Research on Tumstatin in foreign countries has recently been reported. What they mainly focused on was Tumstatin's inhibitory activity against vascular proliferation *in vivo* and *in vitro*. Experiments *in vitro* and *in vivo* identified that 19peptide could inhibit tumor cell proliferation and promote tumor cell apoptosis. It also could inhibit endothelial cell proliferation to some extent. The anti-tumor activity of 19peptide mainly relied on affecting tumor cell directly and partly on inhibiting vascularization. 19peptide will possibly become a new effective tumor therapeutic drug.

Would 19peptide have an equally obvious inhibitory effect on other tumor cells as it does on murine B16 melanoma cells and hepatic carcinoma cells? Would 19peptide have some inhibitory effect on normal somatic cells? Would the efficiency of tumor therapy be able to change with 19peptide for a longer time? These questions have not been answered yet. Further studies will be continued in the future.

Acknowledgements This paper was supported by the National Natural Science Foundation of China (Grant No. 30472035), Heilongjiang Province Natural Science Foundation of China (No. TD2005-21) and Heilongjiang Province Educational Science Foundation of China (No. 11511104).

References

- Colorado P C, Torre A, Kamphaus G (2000). Anti-angiogenic cues from vascular basement membrane collagen. *Cancer Res*, 60(9): 2520–2526.
- Dhanabal M, Ramchandran R, Waterman M J (1999). Endostatin induces endothelial cell apoptosis. *J Biol Chem*, 274(17): 11721–11726.
- Floquet N, Pasco S, Ramont L, Derreumaux P, Laronze J Y, Nuzillard J M, Maquart F X, Alix A J, Monboisse J C (2004). The antitumor properties of the alpha3(IV)-(185-203) peptide from the NC1 domain of type IV collagen (tumstatin) are conformation-dependent. *J Biol Chem*, 279(3): 2091–2100.
- Folkman J (1995). Clinical application of research on angiogenesis. *N Eng J Med*, 333: 1757–1763.
- Kalluri R (2002). Discovery of type IV collagen non-collagenous domains as novel integrin ligands and endogenous inhibitors of angiogenesis. *Cold Spring Harb Symp Quant Biol*, 67: 255–266.
- Kumar C C (2003). Integrin alpha v beta 3 as a therapeutic target for blocking tumor-induced angiogenesis. *Cuf Drug Targets*, 4(2): 123–131.
- Lucas R, Homgren L, Garcia J (1998). Multiple forms of angiostatin induce apoptosis in endothelial cells. *Blood*, 92(12): 4730–4741.
- Maeshima Y, Colorado P C, Kalluri R (2000). Two RGD-independent alpha v beta 3 integrin binding sites on tumstatin regulate distinct anti-tumor properties. *J Biol Chem*, 275(31): 23745–23750.
- Maeshima Y, Colorado P C, Torre A, Holthaus K A, Grunkemeyer J A, Ericksen M B, Hopfer H, Xiao Y, Stillman I E, Kalluri R (2000). Distinct antitumor properties of a type IV collagen domain derived from basement membrane. *J Biol Chem*, 275(28): 21340–21348.

- Maeshima Y, Manfredi M, Reimer C, Holthaus K A, Hopfer H, Chandamuri B R, Kharbanda S, Kalluri R (2001). Identification of the anti-angiogenic site within vascular basement membrane-derived tumstatin. *J Biol Chem*, 276(18): 15240–15248
- Maeshima Y, Sudhakar A, Lively J C, Ueki K, Kharbanda S, Kahn C R, Sonenberg N, Hynes R O, Kalluri R (2002). Tumstatin, an endothelial cell-specific inhibitor of protein synthesis. *Science*, 295(5552): 140–143.
- Maeshima Y, Yerramalla U L, Dhanabal M, Holthaus K A, Barbashov S, Kharbanda S, Reimer C, Manfredi M, Dickerson W M, Kalluri R (2001). Extracellular matrix-derived peptide binds to alpha(v)beta(3) integrin and inhibits angiogenesis. *J Biol Chem*, 276(34): 31959–31968
- O'Reilly M S, Boehm T, Shing Y (1997). Endostatin: an endogenous inhibition of angiogenesis and tumor growth. *Cell*, 88(2): 277–285
- Ortega N, Werb Z (2002). New function roles for non-collagenous domains of basement membrane collagenous. *J Cell Sci*, 115(22): 4201–4214
- Pasco S, Monboisse J C, Kieffer N (2000). The alpha 3(IV)185-203 peptide from noncollagenous domain 1 of type IV collagen interacts with a novel binding site on the beta 3 subunit of integrin alphaV beta 3 and stimulates focal adhesion kinase and phosphatidylinositol 3-kinase phosphorylation. *J Biol Chem*, 275(42): 32999–33007.
- Saus J, Wieslander J, Langeveld J P, Quinones S, Hudson B G (1988). Identification of the Goodpasture antigen as the alpha 3(IV) chain of collagen IV. *J Biol Chem*, 263(26): 13374–13380
- Scappaticci F A (2002). Mechanisms and future directions for angiogenesis-based cancer therapies. *J Clinical Oncolog*, 20(18): 3906–3927
- Scappaticci F A (2003). The therapeutic potential of novel antiangiogenic therapies. *Expert Opin Investig Drugs*, 12(6): 923–932
- Sudhakar A, Sugimoto H, Yang C, Lively J, Zeisberg M, Kalluri R (2003). Human tumstatin and human endostatin exhibit distinct anti-angiogenic activities mediated by alpha v beta 3 and alpha 5 beta 1 integrins. *Proc Natl Acad Sci USA*, 100(8): 4766–4771.
- Yu Qiong, Zhou Lingyun, Lin Xuesong, Xu Jianyong, Wang Shujing, Liu Xinghan (2004). Expression, purification and activity of recombinant human osteogenic growth peptide (rhOGP). *Chin J Biochem Mol Biol*, 20(4): 467–472 (in Chinese)